Khan et al. BMC Complementary and Alternative Medicine (2018) 18:48
DOI 10.1186/s12906-018-2116-x

BMC Complementary and Alternative Medicine

RESEARCH ARTICLE Open Access

Computational investigations of physicochemical, pharmacokinetic, toxicological properties and molecular docking of betulinic acid, a constituent of *Corypha taliera* (Roxb.) with Phospholipase A2 (PLA2)

Mohammad Firoz Khan[1], Nusrat Nahar[1], Ridwan Bin Rashid[1], Akhtaruzzaman Chowdhury[2] and Mohammad A. Rashid[3*]

Abstract

Background: Betulinic acid (BA) is a natural triterpenoid compound and exhibits a wide range of biological and medicinal properties including anti-inflammatory activity. Therefore, this theoretical investigation is performed to evaluate (a) physicochemical properties such as acid dissociation constant (pKa), distribution coefficient (logD), partition coefficient (logP), aqueous solubility (logS), solvation free energy, dipole moment, polarizability, hyperpolarizability and different reactivity descriptors, (b) pharmacokinetic properties like human intestinal absorption (HIA), cellular permeability, skin permeability (P_{Skin}), plasma protein binding (PPB), penetration of the blood brain barrier (BBB), (c) toxicological properties including mutagenicity, carcinogenicity, risk of inhibition of hERG gene and (d) molecular mechanism of anti-inflammatory action which will aid the development of analytical method and the synthesis of BA derivatives.

Methods: The physicochemical properties were calculated using MarvinSketch 15.6.29 and Gaussian 09 software package. The pharmacokinetic and toxicological properties were calculated on online server PreADMET. Further, the molecular docking study was conducted on AutoDock vina in PyRx 0.8.

(Continued on next page)

* Correspondence: rashidma@du.ac.bd
[3]Department of Pharmaceutical Chemistry, University of Dhaka, Dhaka 1000, Bangladesh
Full list of author information is available at the end of the article

(Continued from previous page)

Results: The aqueous solubility increased with increasing pH due to the ionization of BA leading to decrease in distribution coefficient. The solvation energies in water, dimethyl sulfoxide (DMSO), acetonitrile, *n*-octanol, chloroform and carbon tetrachloride were − 41.74 kJ/mol, − 53.80 kJ/mol, − 66.27 kJ/mol, − 69.64 kJ/mol, − 65.96 kJ/mol and − 60.13 kJ/mol, respectively. From the results of polarizability and softness, it was clear that BA is less stable and hence, kinetically more reactive in water. BA demonstrated good human intestinal absorption (HIA) and moderate cellular permeability. Further, BA also exhibited positive CNS activity due to high permeability through BBB. The toxicological study revealed that BA was a mutagenic compound but noncarcinogenic in mice model. Moreover, molecular docking study of BA with PLA2 revealed that BA interacts with GLY22 & GLY29 through hydrogen bond formation and LEU2, PHE5, HIS6, ALA17, ALA18, HIS47 and TYR51 through different types of hydrophobic interactions. The binding affinity of BA was − 41.00 kJ/mol which is comparable to the binding affinity of potent inhibitor 6-Phenyl-4(R)-(7-Phenyl-heptanoylamino)-hexanoic acid (BR4) (− 33.89 kJ/mol).

Conclusions: Our computed properties may assist the development of analytical method to assay BA or to develop BA derivatives with better pharmacokinetic and toxicological profile.

Keywords: Physicochemical properties, Solvation free energy, Polarizability, Pharmacokinetic, Toxicology, Carcinogenic, Molecular docking

Background

Betulinic acid (BA), (3β-hydroxy-lup-20(29)-en-28-oic acid) (Fig. 1) is a natural pentacyclic lupane type triterpenoid compound and exhibits a wide range of biological and medicinal properties such as antivenom [1], anti-HIV [2, 3], antibacterial [2], antimalarial [4], anti-inflammatory [5–7] anthelmintic [8], antinociceptive [9], anti-HSV-1 [10, 11] and anticancer activities [12–14]. It is abundantly distributed throughout the plant kingdom [15]. The birch tree (*Betula* spp., Betulaceae) is one of the most widely reported sources of BA which can be obtained in considerable quantities [16, 17]. BA can also be isolated from various sources including *Corypha taliera* [18], *Ziziphus* spp. (Rhamnaceae) [19, 20], *Syzygium* spp. (Myrtaceae) [21], *Diospyros* spp. (Ebenaceae) [22, 23] and *Paeonia* spp. (Paeoniaceae) [24]. Betulin, the reduced form of BA, was one of the first natural products to be isolated from the bark of the white birch, *Betula alba* [25].

BA was shown to exert its diverse pharmacological activities with variable median inhibitory concentrations (IC_{50}) such as anticancer activity by inhibiting DNA Topoisomerases (Topos) II at IC_{50} of 56.12 μM [26], anti-HIV activity at IC_{50} of 23.65 μM [27], anti-malarial activity at IC_{50} of 56.71 μM [28], anti-fungal property at IC_{50} of 14.23 μM [29], anti-protozoal activity at IC_{50} of 50 μM [30].

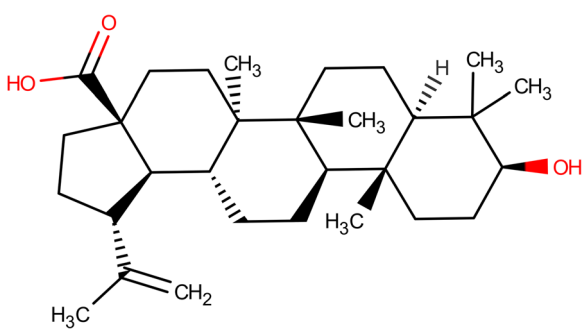

Fig. 1 Structure of betulinic acid

BA also inhibited DNA polymerase beta at IC_{50} of 30.65 μM [31], protein tyrosine phosphatase 1B (PTP1B) at IC_{50} value of 1.5 μM [32], inhibited *T. brucei* GAPDH COX-1, COX-2 and LT formation in vitro with IC_{50} values of 240 μM [33], > 125 μM, > 125 μM and 102.2 μM [34], respectively. BA displayed potent anti-inflammatory activity by inhibiting Phospholipase A2 (PLA2) and showed 30% and 40% inhibition of PLA2 at concentrations of approximately 2.5 and 5 μM, respectively [5].

Earlier studies showed that BA exhibited anti-inflammatory activity by inhibiting TNF- alpha and increasing the production of anti-inflammatory cytokine IL-10 [35]. Kim and colleagues demonstrated that betulinic acid exerted its anti-inflammatory activity by inhibiting the nuclear factor-kappa beta pathway, production of nitric oxide (NO), prostaglandin E2 (PGE2), tumor necrosis factor- alpha, interleukin-6 (IL-6), and interleukin-1 beta levels [36]. Anti-inflammatory activity was also seen in encephalitogenic T cells where betulinic acid inhibited IL-17 and IFN-γ production [37]. Arachidonoyl trifluoromethyl ketone, bromoenol lactone, varespladib, varespladib methyl, ecopladib, efipladib, giripladib, pyrrophenone, pyrroxyphene, FPL67047XX, inhibitor 22, amide 23 (GK115), 2-oxoamides, 1,3-disubstituted propan-2-ones are all synthetic phospholipase A2 inhibitors that have been used for clinical cases [38]. Among natural compounds, extracts of curcumin, *Ginkgo biloba* and *Centella asiatica* have demonstrated to be phospholipase A2 inhibitors and have even been used to treat neurological disorders characterized by neuroinflammation [38]. Bernard and colleagues experimentally

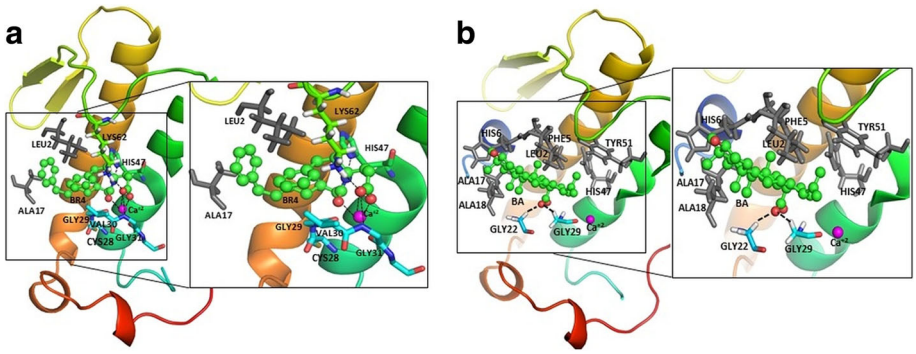

Fig. 2 Interaction of (**a**). BR4 (green) and (**b**). BA (green) with PLA2 visualized in pymol. The calcium ion (Ca^{+2}) is presented as magenta color sphere. Black dash indicates H bonding. Residues involve in hydrophobic interactions are shown in gray color

proved that betulin and betulinic acid were potent phospholipase A2 inhibitors [5].

Phospholipase A2 (PLA2) hydrolyzes the membrane glycerophospholipids and releases arachidonic acid eventually leading to the production of pro-inflammatory mediators such as leukotrienes, prostaglandins, platelet activating factors (PAF) [39]. Thus, inhibiting PLA2 activity and hence regulating the production of pro-inflammatory mediators for the development of therapeutics against inflammatory diseases [40, 41] is a plausible approach. However, the PLA2 exists in two isoforms [40, 42], which includes the low molecular weight (14 kDa) Ca^{+2} dependent extracellular PLA2 found in mammalian pancreases, several snake venoms, human platelets, human placentas, rheumatoid synovial fluids [43] and the high molecular weight (85 kDa) cytosolic PLA2 [44]. Convincing evidence suggests that the14 kDa PLA2 might be a potential target for the modulation of inflammatory diseases [40], here we have reported the molecular docking study of BA against human secretory (14 kDa) PLA2 (1KQU) to explore the molecular basis of anti-inflammatory action of BA.

Few computational and theoretical studies of BA have been reported. BA associates with human serum albumin via hydrogen bond with PHE206 & GLU354 and hydrophobic interactions with PHE206, ARG209, ALA210, ALA213, LEU327, GLY328, LEU331, ALA350 and LYS351, in the sub-domain IIA and IIB of the large hydrophobic cavity [45].

In this investigation, computational studies have been carried out to evaluate (a) physical and chemical properties such as acid dissociation constant (pKa), distribution coefficient (logD), partition coefficient (logP), aqueous solubility (logS), solvation free energy, dipole moment, polarizability, hyperpolarizability and different reactivity descriptors (chemical hardness, softness, chemical potential, electronegativity, electrophilicity index), (b) pharmacokinetic properties like human intestinal absorption (HIA), cellular permeability using Caco-2 cell model, skin permeability (P_{Skin}), plasma protein binding (PPB),

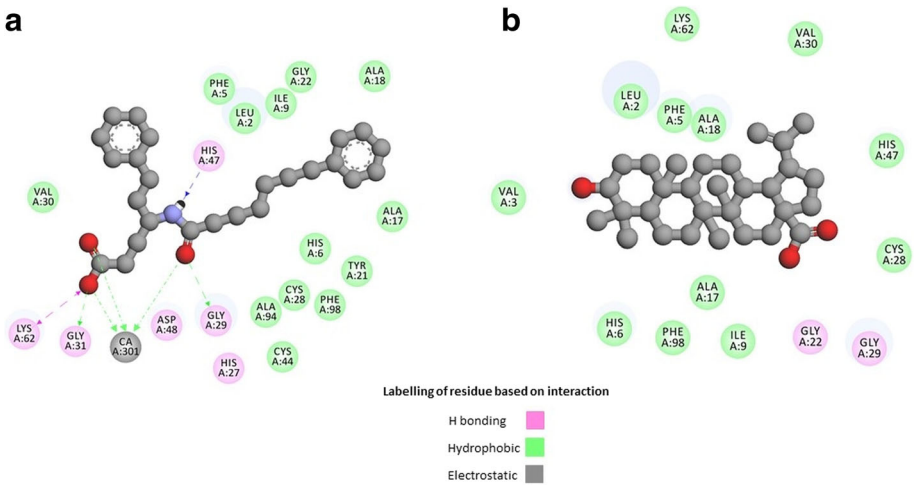

Fig. 3 Interaction of (**a**). BR4 (gray) and (**b**). BA (gray) with PLA2 visualized in Drug Discovery studio

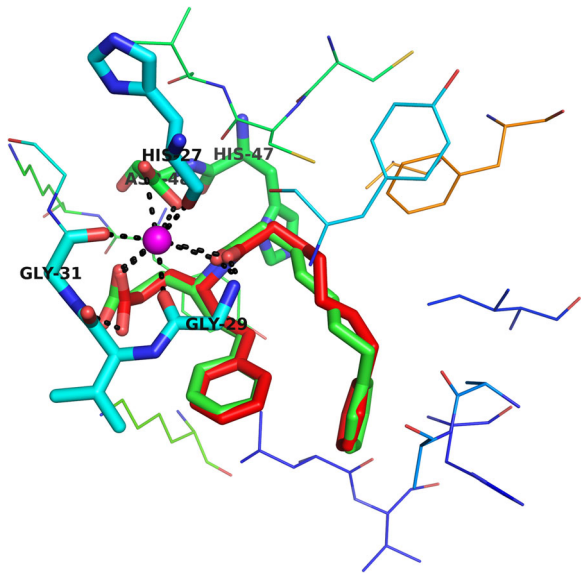

Fig. 4 The superimposition of the best docking structure with the X-ray structure visualized in PyMOL; ( ) experimental ligand, ( ) docked ligand

penetration of the blood brain barrier (BBB), (c) toxicological properties including mutagenicity, carcinogenicity, risk of inhibition of human ether-a-go-go-related (hERG) gene and (d) molecular mechanism of anti-inflammatory action of BA. The purpose of this study was to investigate the physicochemical, pharmacokinetic and toxicological properties and to correlate the calculated physicochemical properties with the absorption and distribution profile of BA. These in silico investigations will provide an insight for the development of analytical method to assay BA [46] or to develop BA derivatives with better pharmacokinetic & toxicological profile and having more potent anti-inflammatory activity.

Methods

Computational methods

The acid dissociation constant (pKa), distribution coefficient (logD), partition coefficient (logP) and aqueous solubility (logS) of betulinic acid (BA) over the pH range of 0.0 to 14.0at 298 K were calculated using MarvinSketch 15.6.29 (ChemAxon, Hungary) (http://www.chemaxon.com). The consensus logP method was applied to calculate distribution coefficient of the molecule.

The rapid progress in computational methods such as Gaussian family of methods (G1, G2, G2MP2, G3) and complete basis set extrapolation (CBS) method enable researchers to perform highly sophisticated calculations of enthalpies and thermochemical properties with minor errors in comparison to experimental data [47–51]. However, these methods are computationally very expensive. An alternative to these high cost calculations is the use of density functional theory (DFT) methods. Previous report revealed that [52] calculation of geometries (bond length, bond angle and dihedral angle) and thermochemical properties using DFT/B3LYP level of theory showed better agreement with the experiments. So, in the current investigation, the calculation of solvation free energy, dipole moment, polarizability, hyperpolarizability and global reactivity descriptor properties such as the chemical hardness, softness, chemical potential, electronegativity, electrophilicity index were conducted in gas phase and in different solvents namely water, dimethyl sulfoxide (DMSO), acetonitrile, *n*-octanol, chloroform and carbon tetrachloride with the B3LYP/6-31G(d) level of theory implemented in Gaussian 09 software package [53].

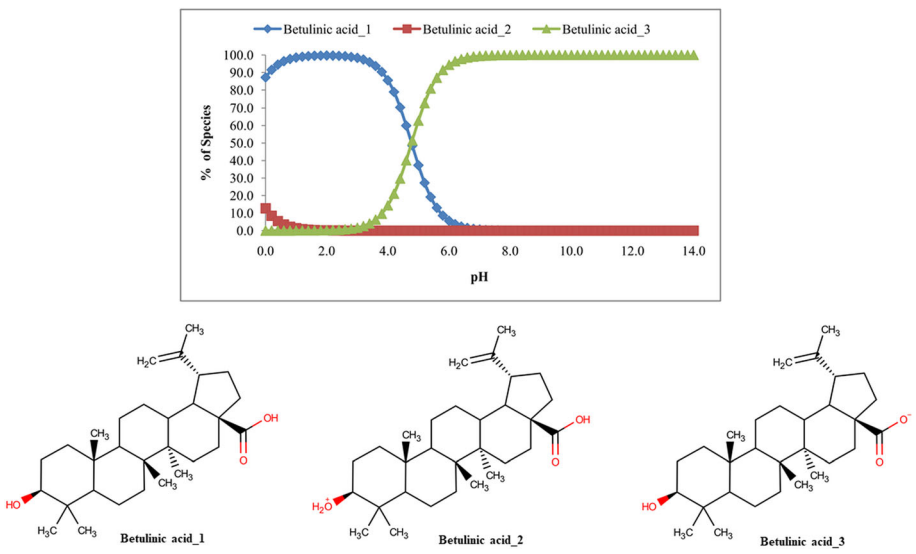

Fig. 5 Microspecies distribution (%) of betulinic acid

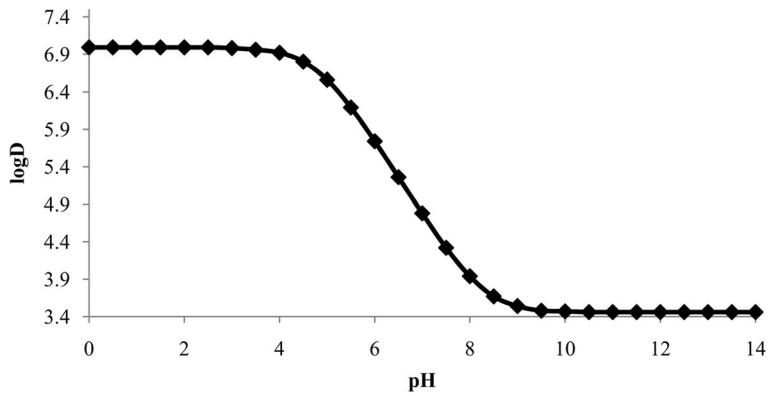

Fig. 6 Distribution coefficient (logD) of betulinic acid over the pH range of 0.0 to 14.0

All calculations were conducted using the optimized geometry which was confirmed by the absence of imaginary frequency in the lowest energy state of the molecule. The Solvation Model on Density (SMD) [54] was used for all calculations involving the solvents. All calculations involving solvation were performed using the optimized solution-phase structures.

The pharmacokinetic and toxicological properties were calculated using online server PreADMET (https://preadmet.bmdrc.kr/). The pharmacokinetic properties such as human intestinal absorption (HIA), in vitro cellular permeability using Caco-2 cell model, skin permeability (P_{Skin}), plasma protein binding (PPB) and penetration of the blood-brain barrier (BBB), interaction with P-glycoprotein (Pgp) and metabolism (both phase I and phase II) were calculated and predicted. In addition, BA was virtually screened to evaluate toxicological properties such as mutagenicity, carcinogenicity and risk of inhibition of human ether-a-go-go-related (hERG) gene.

Molecular docking study

Preparation of target protein X-ray structure

The first step of docking study is to select an appropriate X-ray crystal structure of the target protein that is already bound to its known ligand. This is because during docking, software searches complementary binding site/(s) for ligand within the search space of the target protein. That's why ligand bound conformation of protein structure is the prerequisite to perform molecular docking. Moreover, the structure should be solved with a reasonable accuracy which is reflected in the statistics for data collection and processing of X-ray crystal structure. In addition, refinement statistics such as R_{work}/R_{free}, RMS deviation from ideality (bonds and angles) and validation parameters including Ramachandran outliers, rotamer outliers, bad bond count or bad angle count etc. also indicate the quality of the model structure. In our current investigation, we have selected the crystal structure of secretory PLA2 complexed with 6-Phenyl-4(R)-(7-Phenyl-heptanoylamino)-hexanoic acid (BR4) (PDB code: 1KQU) [55] since the structure was solved at 2.1 Å resolution with R_{work}/R_{free} of 0.209/0.240 and the validation parameters indicates good quality of the model structure. Water molecules and hetero atoms were then removed from the protein using PyMOL (Version 1.7.4.4, Schrödinger). Energy minimization was performed by applying YASARA force field level of theory in YASARA Energy Minimization Server (http://www.yasara.org/minimizationserver.htm).

Table 1 Comparison of partition coefficient of betulinic acid

	logP
MarvinSketch 15.6.29	6.64
Experimental (40)	6.61
Experimental (41)	6.85

Preparation of ligands

The structure of the BR4 and BA were drawn and optimized in Gaussian 09 [53] with density functional theory (DFT) at the B3LYP/6-31G(d) level of theory. The optimized structures of ligands (BR4 and BA) were saved in PDB format for docking study.

Protein-ligand docking

Several virtual screening tools are available to perform molecular docking such as BINDSURF, METADOCK, Lead Finder, FlexScreen, AutoDock vina etc. Scoring functions implemented in these softwares calculate the protein-ligand interactions energy by computing electrostatic, Van der Waals and hydrogen bonding terms [56–60]. In addition to these scoring functions AutoDock vina also calculates the hydrophobic interactions [60] which is crucial for calculating the interaction energies of protein and hydrophobic ligand. Since BA is hydrophobic in nature, we used AutoDock vina

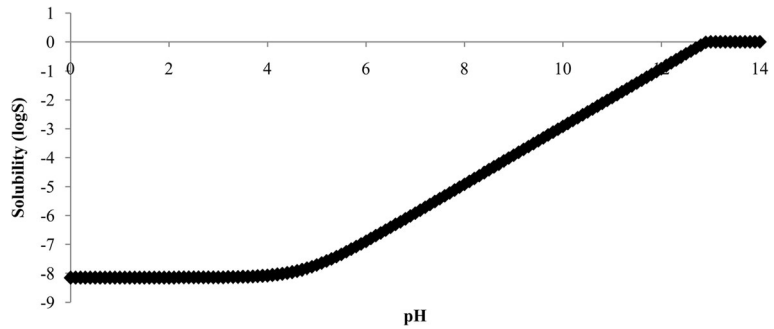

Fig. 7 Solubility (logS) of betulinic acid over the pH range of 0.0 to 14.0

to explore not only the electrostatic, Van der Waals and hydrogen bonding but also the hydrophobic interactions.

The docking of target protein with the ligands was conducted using AutoDock vina [60] in PyRx 0.8 (https://pyrx.sourceforge.io/). Docking study was performed to get a set of possible conformations and orientations for the ligand at the binding site. Using PyRx software, the PLA2 and ligands were prepared after which docking was conducted using a grid whose center was (56.5961, 34.0180, 42.4808) and the dimensions were (25.00, 25.00, 25.00) Å. During the docking analysis, the drug molecules were flexible and the macromolecule was kept rigid. Ligand displaying the lowest binding affinity and ability to bind in the binding pocket of protein was chosen as the best conformation. The interactions of different residues of protein with ligands such as hydrogen bonds, electrostatic interactions, hydrophobic interactions and bond distances were analyzed by PyMOL and Discovery Studio visualizer v4.0.100.13345 (Figs. 2 and 3).

Before docking of BA, the protocol was validated by re-docking BR4 into the binding pocket of 1KQU to get the docked pose and root mean square deviation (RMSD). The result revealed that the first pose of BR4 almost superimposed (RMSD of heavy atoms constituting the backbone of molecule is 0.5271) with the experimental crystal structure of BR4 (Fig. 4). Thus, the docking method has reasonable accuracy and reproducibility and can be used for further docking experiments.

Table 2 Solvation free energy (kJ/mol) of betulinic acid in different solvents with SMD

Medium (dielectric constant)	Solvation free energy (kJ/mol)
Water (78.3)	−41.74
DMSO (46.8)	−53.80
Acetonitrile (35.7)	−66.27
n-Octanol (9.9)	− 69.64
Chloroform (4.7)	−65.96
Carbon tetrachloride (2.2)	−60.13

Results and discussion

Calculation of pKa

The calculation of pKa revealed that BA has two ionized species along with the unionized form (Fig. 5). It is clear from the figure that non-ionized form (Betulinic acid_1) predominates over the pH range of 0.0 to 4.6 whereas the betulinate form (Betulinic acid_3) dominates from pH 4.8 to 14.0. However, small amount of Betulinic acid_2 was present over the pH of 0.0 to 2.4.

Distribution (logD) coefficient and partition (logP) coefficient

The logD was calculated using consensus method implemented in MarvinSketch 15.6.29. The logD vs pH of BA is presented in Fig. 6. The logD value decreases with increasing pH of the solution suggesting that the prevalence of the unionized form of BA decreases and the ionized form (betulinate) increases with increasing pH of the solution. This result is in accordance with the calculation of pKa.

The partition coefficient (logP) of BA was also computed and presented in Table 1. The logP calculated in MarvinSketch 15.6.29 was 6.64 whereas the experimental logP of BA were reported as 6.61 [61] and 6.85 [62].

Table 3 Dipole moment (Debye, (D)) of betulinic acid in gas phase and in different solvents using SMD

Medium (dielectric constant)	Dipole Moment (D)
Gas	2.98
Water (78.3)	5.13
DMSO (46.8)	4.50
Acetonitrile (35.7)	4.53
n-Octanol (9.9)	4.54
Chloroform (4.7)	3.96
Carbon tetrachloride (2.2)	3.46

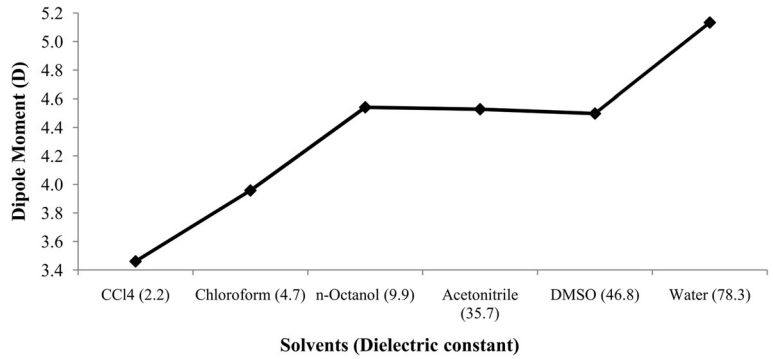

Fig. 8 Effect of solvent polarity on dipole moment (D) of betulinic acid

Aqueous solubility (logS)

The aqueous solubility of BA in terms of logS is presented in Fig. 7. The figure indicates that the solubility increases with increasing pH of the solution. However, the intrinsic solubility of BA was found − 7.34 (0.000000046 mol/L) and the aqueous solubility at pH 7.4 was − 4.79 (0.000016 mol/L) indicating that BA is practically insoluble in water.

Solvation free energy

The solvation free energies of BA were calculated with the SMD model [54] The values are summarized in Table 2. The solvation energies of BA in water, DMSO, acetonitrile, *n*-octanol, chloroform and carbontetrachloride were − 41.74 kJ/mol, − 53.80 kJ/mol, − 66.27 kJ/mol, − 69.64 kJ/mol, − 65.96 kJ/mol and − 60.13 kJ/mol, respectively. It could therefore be concluded that solvation free energy increases with decreasing polarity of polar nonprotic solvent (DMSO and acetonitrile). The highest value of solvation energy was in non-polar protic solvent (*n*-octanol). The free energy decreases with decreasing polarity of non-polar aprotic solvent (chloroform and carbon tetrachloride). Thus, it could be stated that BA associates with non-polar portion (hydrocarbon chain of *n*-octanol) via hydrophobic interactions. Electrostatic interactions might arise due to the association of the carboxyl group of BA with the polar portion (hydroxyl group of *n*-octanol) (Table 5).

Dipole moment

The dipole moment of BA is found to be higher in different solvents than that of the gas phase. Table 3 presents the dipole moments computed in the gas phase and different solvents (water, DMSO, acetonitrile, *n*-octanol, chloroform and carbon tetrachloride) at the B3LYP level of theory with 6-31G(d) basis set using SMD solvation model. The dipole moments were 2.98D, 5.13D, 4.50D, 4.53D, 4.54D, 3.96D and 3.46D in the gas phase, water, DMSO, acetonitrile, *n*-octanol, chloroform and carbon tetrachloride, respectively. Therefore, increasing dielectric constant of the solvent is accompanied by a gradual increase in the dipole moment. In other words, the dipole moment increases with the increasing polarity of the solvent (Fig. 8).

Polarizability and first order hyperpolarizability

The polarizability(α) of BA was calculated using the following equation:

$$\alpha = \frac{1}{3}\left(\alpha_{xx} + \alpha_{yy} + \alpha_{zz}\right)$$

The quantities α_{xx}, α_{yy} and α_{zz} are known as principal values of polarizability tensor.

The calculated polarizability of BA in different solvents is presented in Table 4, which showed that polarizability (α_{tot}) ranged from 351.90 to 448.67 a.u. The plot of polarizability vs. solvent is shown in Fig. 9. It is clear

Table 4 Effect of solvent polarity on polarizability (a.u.) and first order hyperpolarizability (a,u)

Medium (dielectric constant)	α_{xx}	α_{yy}	α_{zz}	α_{tot}	β_x	β_y	β_z	β_{tot}
Gas Phase	355.73	300.52	260.89	305.72	103.92	−121.26	−37.58	164.06
Water (78.3)	447.54	459.46	439.01	448.67	154.68	− 170.92	−87.52	246.57
DMSO (46.8)	441.82	450.17	428.25	440.08	132.92	− 155.98	−68.48	216.07
Acetonitrile (35.7)	442.00	448.66	425.71	438.79	130.61	−155.78	−70.89	215.30
n-Octanol (9.9)	434.46	426.93	394.48	418.62	139.39	− 157.93	−74.51	223.43
Chloroform (4.7)	418.61	395.58	356.17	390.12	124.74	− 146.22	−58.57	200.93
Carbon tetrachloride (2.2)	393.70	352.38	309.63	351.90	117.66	− 134.29	−46.43	184.48

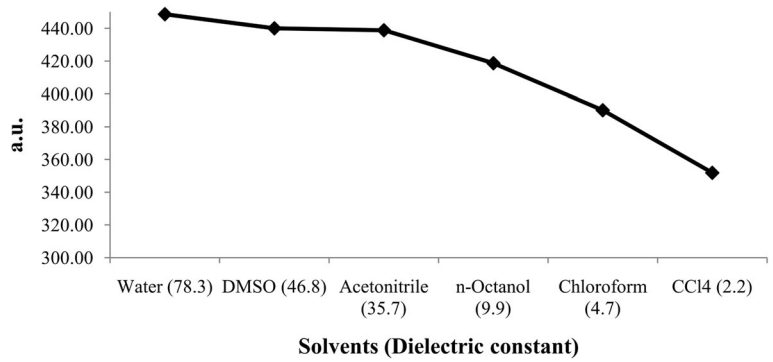

Fig. 9 Effect of solvent polarity on polarizability of betulinic acid

from the figure that the polarizability gradually increases when going from lower to higher dielectric constant. This suggests that the kinetic reactivity of BA increases with increasing polarity of the solvent [63].

The first order hyperpolarizability (β_{tot}) is the measure of the nonlinear optical activity and can be calculated using the following equation:

$$\beta_{tot} = \left(\beta_x^2 + \beta_y^2 + \beta_z^2\right)^{1/2}$$

Where,

$$\beta_x = \beta_{xxx} + \beta_{xyy} + \beta_{xzz}$$
$$\beta_y = \beta_{yyy} + \beta_{xxy} + \beta_{yzz}$$
$$\beta_z = \beta_{zzz} + \beta_{xxz} + \beta_{yyz}$$

The β_{tot} for different solvents was listed in Table 4, which displayed that the hyperpolarizability in different solvents ranged from 184.48 to 246.57 a.u. Moreover, the hyperpolarizability increases as the dielectric constant increases except for non-polar protic *n*-octanol where the hyperpolarizability is higher than that of acetonitrile and DMSO (Fig. 10).

Global reactivity descriptors

The highest occupied molecular orbital-lowest unoccupied molecular orbital (HOMO-LUMO) energy gap represents the stability or reactivity of molecules. Higher energy gap indicates greater stability and vice versa. The values of HOMO-LUMO energy gap in various solvents are presented in Table 5 and their trend is shown in Fig. 11. From Fig. 11, it is clear that the HOMO-LUMO energy gap is the highest in DMSO and acetonitrile, indicating greater stability of BA in these solvents, however lowest HOMO-LUMO energy gap was found in water meaning the titled molecule is less stable and hence, more reactive in water which is in agreement with calculated polarizability, chemical hardness and softness. The Table 5 and Fig. 11 suggest that the molecule is stabilized with decreasing polarity of the solvent i.e. the molecule is less likely to be kinetically reactive.

The global chemical reactivity descriptors such as softness, hardness, chemical potential and electrophilicity index can be calculated from the HOMO-LUMO energy gap of a molecule [64–68]. Using Koopman's theorem for closed-shell molecules the hardness (η), chemical potential(μ), electronegativity (χ) and softness (S) are calculated according to the following equation:

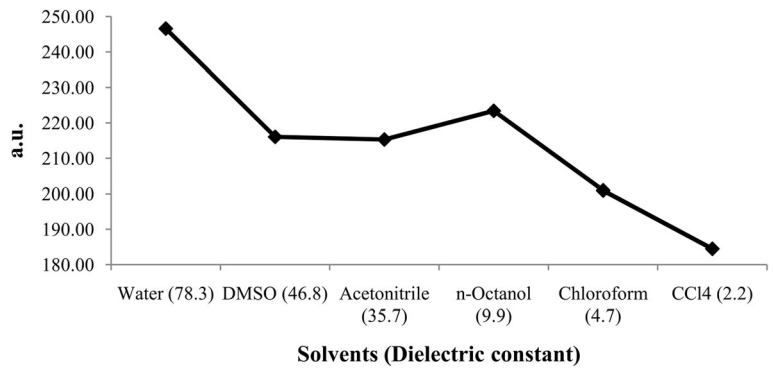

Fig. 10 Effect of solvent polarity on first order hyperpolarizability of betulinic acid

Table 5 Molecular Orbital Energy (eV) (HOMO and LUMO) of betulinic acid in different solvents with SMD

Medium (dielectric constant)	Molecular Orbital Energy (eV)		
	HOMO	*LUMO*	*ΔE*
Gas Phase	−6.305	0.133	6.438
Water (78.3)	−6.262	0.116	6.378
DMSO (46.8)	−6.243	0.321	6.564
Acetonitrile (35.7)	−6.244	0.321	6.565
n-Octanol (9.9)	−6.241	0.201	6.441
Chloroform (4.7)	−6.222	0.286	6.508
Carbon tetrachloride (2.2)	−6.229	0.251	6.480

$$\eta = \frac{I-A}{2}$$

$$\mu = -\frac{I+A}{2}$$

$$\chi = \frac{I+A}{2}$$

$$S = \frac{1}{\eta}$$

Where

Ionization potential, $I = -E_{HOMO}$

Electron affinity, $A = -E_{LUMO}$

The electrophilicity index (ω) is calculated according to equation derived (by Parr et al., [68]) [58] as follows:

$$\omega = \frac{\mu^2}{2\eta}$$

The molecular properties of BA in different solvents are presented in Table 6. No systematic trend was found in the case of chemical hardness & softness, chemical potential, electronegativity and electrophilicity index. However, the highest chemical softness, electronegativity and electrophilicity index was found in water (polar protic) followed by *n*-octanol (non-polar aprotic) and carbon tetrachloride (non-polar aprotic).

Pharmacokinetic study

Pharmacokinetic studies such as absorption, distribution and metabolism of BA was done by using the web based application PreADMET (https://preadmet.bmdrc.kr/). The calculated absorption, distribution and metabolism parameters are presented in Table 7.

The calculated human intestinal absorption HIA of BA (Table 7) was found to be 95.996% which suggests that BA is well absorbed through the intestinal cell [69]. BA was moderately permeable since values for absorption through Caco-2 cell ($P_{Caco\text{-}2}$) was 21.86 [70]. The skin permeability (P_{Skin}) is a vital parameter for assessment of drugs and chemical that might require transdermal administration [71]. BA was found to be impermeable through skin since a calculated P_{Skin} was − 2.11 encountered which proves BA is not permeable through the skin.

The distribution properties were assessed by measuring the brain to blood partitioning (C_{brain}/C_{blood}) and plasma protein binding (PPB). Generally, compounds with more than 90% of PPB are classified as strongly bound chemicals whereas less than 90% are weakly bound chemicals (https://preadmet.bmdrc.kr/adme-prediction/). The calculated value of PPB for BA was 100.00% indicating BA is a strongly bound chemical and hence, the free form of BA will be less available in the systematic circulation. Based on C_{brain}/C_{blood} ratio all chemicals fall under three categories namely high absorption to CNS (C_{brain}/C_{blood} value more than 2.0), moderate absorption to CNS (C_{brain}/C_{blood} value within 2.0–0.1) and low absorption to CNS (C_{brain}/C_{blood} value less than 0.1) [72]. The ratio of C_{brain}/C_{blood} (8.20) suggests high absorption of BA to CNS indicating higher ability to cross blood brain barrier (BBB).

The exchangeable fraction (sum of unbound fraction and fraction dissociated from the protein) of drug determines the amount of drug that will penetrate the BBB

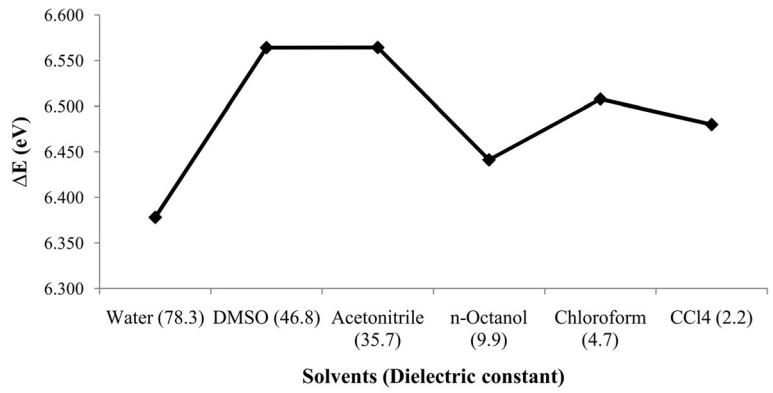

Fig. 11 Effect of solvent polarity on HOMO-LUMO energy gap of betulinic acid

Table 6 Effect of solvent polarity on molecular properties of betulinic acid

Medium (dielectric constant)	Chemical hardness (η)	Softness (S)	Chemical potential (μ)	Electronegativity (χ)	Electrophilicity index (ω)
Gas Phase	3.219	0.311	−3.086	3.086	1.479
Carbon tetrachloride (2.2)	3.240	0.309	−2.989	2.989	1.379
Chloroform (4.7)	3.254	0.307	−2.968	2.968	1.354
n-Octanol (9.9)	3.221	0.310	−3.020	3.020	1.416
Acetonitrile (35.7)	3.282	0.305	−2.962	2.962	1.336
DMSO (46.8)	3.282	0.305	−2.961	2.961	1.336
Water (78.3)	3.189	0.314	−3.073	3.073	1.480

[73]. Besides, Pardridge and colleagues have reported the permeation of protein-bound compounds through the BBB [74–76]. Since BA is a strongly protein bound chemical (100%) so it could be assumed that BA will penetrate the BBB either due to the fraction dissociated from the plasma protein or as a protein-bound form or both.

P-glycoprotein (Pgp) is the product of the multi drug resistance (MDR) gene and an ATP dependent efflux transporter that affects the absorption, distribution and excretion of clinically important drugs [77]. Over-expression of this protein, which may result in MDR is a major cause of the failure of cancer chemotherapy, and decreased efficacy of antibiotics [78, 79]. The prediction of Pgp substrates, which facilitates early identification and elimination of drug candidates of low efficacy or high potential of MDR [80, 81]. Identifying molecules that interact with Pgp transporters is important for drug discovery, but it is commonly determined through laborious in vitro and in vivo studies [82]. Computational classification model can be used to screen molecules and predict the likeliness to be substrate for Pgp [82]. The in silico screening revealed that BA is a dual inhibitor and substrate for Pgp like quinidine [83]. This is because due to complex modulatory interactions with the Pgp which make BA to function as combination of substrate and inhibitor [83].

Table 7 Absorption, distribution and metabolism of betulinic acid

Absorption			
HIA (%)	P_{Caco-2} (nm/s)		P_{skin}
96.00	21.86		−2.11
Distribution			
PPB (%)	C_{brain}/C_{blood}	P-Glycoprotein (Inhibition)	P-Glycoprotein (Substrate)
100.00	8.20	Inhibitor	Substrate
Metabolism			
Phase I		Phase II	
Enzyme	*Inhibitor/ Substrate*	*Enzyme*	*Substrate/ Non-substrate*
Cytochrome P450 2C19 (Inhibitor)	Non	UDP-glucuronosyltransferase (UGT)	Non-substrate
Cytochrome P450 2C9 (Inhibitor)	Inhibitor	Sulfotransferase (SULT)	Non-substrate
Cytochrome P450 2D6 (Inhibitor)	Non		
Cytochrome P450 2D6 (substrate)	Non		
Cytochrome P450 3A4 ((Inhibitor)	Inhibitor		
Cytochrome P450 3A4 (substrate)	Substrate		

The computed metabolism of BA (Table 7) displayed that it is an inhibitor of CYP2C9 and a dual inhibitor and substrate for CYP3A4 due to complex modulation of CYP3A4 in phase I reaction. In phase II reaction BA is neither a substrate for UDP-glucuronosyltransferase (UGT) nor sulfotransferase (SULT).

Toxicological study

The PreADMET server (https://preadmet.bmdrc.kr/) was used to evaluate the carcinogenicity of BA. It was found that although BA is mutagenic but it demonstrated non-carcinogenicity in mice. On the other hand, BA is unlikely to be an inhibitor of human ether-a-go-go-related (hERG) gene (low risk). Inhibition of the hERG gene has been linked to long QT syndrome [84]. The results have been in summarized in Table 8.

Protein optimization

YASARA Energy Minimization Server (http://www.yasara.org/minimizationserver.htm) [85] was used to optimize the structure of PLA2. This server utilizes a

Table 8 Toxicological properties of betulinic acid

Mutagenicity (Ames test)	Carcinogenicity in Mouse	hERG (Inhibition)
Mutagenic	Negative	Low risk

new partly knowledge-based all atom force field derived from Amber, whose parameters have been optimized to attain the protein structure as close as to its native structure with maximum accuracy [85]. The simulation was performed in a water sphere containing ions.

The structure validation Z-scores and force field energies before and after the minimization are displayed in Table 9. The energies of the structure before and after optimization were − 68,549.6 and − 83,729.2 kJ/mol, respectively. This indicates that the protein structure was stabilized by an amount of − 15,179.6 kJ/mol. In addition, the structure validation Z-scores of before and after optimization was − 0.1 and 1.15 indicating good optimization of the target protein. The structure of PLA2 after energy minimization in a water sphere is presented in Fig. 11. PyMOL (Version 1.7.4.4, Schrödinger) was used to evaluate the root mean square deviation (RMSD) between the initial and final structure of PLA2 which was found to be 0.363.

Molecular docking

Molecular docking of BA was carried out with human PLA2 using AutoDock Vina, to identify and understand the binding mode of BA and the intermolecular interactions with the target protein. All reported PLA2 inhibitors possess three key enzyme binding components such as Ca^{+2} binding oxygen atom, a HIS47 binding H-bond donor and a hydrophobic component that bind the active site of the enzyme [55]. So, PLA2 inhibitors should form electrostatic interactions with Ca^{+2} ion, H bond formation with the catalytic HIS47 and different types of hydrophobic interactions with hydrophobic residues which line the active site cavity of the enzyme. In addition, the inhibitors should interact and displace the HIS6; a unique residue to human PLA2 enzyme [55]. From our docking study, it was found that BA interacts with PLA2 at a binding affinity of − 41.00 kJ/mol whereas for BR4 it was − 33.89 kJ/mol. BA lies deep within the active site activity and makes numerous close contacts (< 5.4 Å) with the enzyme through hydrogen bond formation with GLY22 & GLY29 and hydrophobic interactions with the LEU2, PHE5, HIS6, ALA17, ALA18, TYR51 and the catalytic residue HIS47 (Figs. 2 and 3 and Table 10). However, no interactions of BA with calcium were observed as it was found in case of bovine PLA2 [5]. Therefore, BA has the ability to interact with the catalytic residue HIS47 and the base forming residue HIS6 of human PLA2.

Table 9 Optimization parameter of phospholipase A2 (1KQU)

	Force field energy (kJ/mol)	Structure validation Z-score	RMSD of initial and final structure
Before optimization	−68,549.6	−0.1	0.363
After optimization	−83,729.2	1.15	
Difference (Δ)	−15,179.6	1.25	

On the other hand, the standard compound BR4 forms hydrogen bonding with LYS62, HIS47, GLY29, GLY31, CYS28, VAL30 and LYS62. Different types of hydrophobic interactions were also displayed by BR4 with GLY29-VAL30, LEU2 and ALA1. Moreover, BR4 exhibited attractive electrostatic interactions with Ca^{+2} ions.

Binding affinity and in vitro inhibitory activity

A comparison was made between the binding affinities and in vitro inhibitory activities (IC_{50}) of LY 311727, Manoalide, Indomethacin, Manoalogue, Aristolochic Acid and 1,1,1-Trifluoro-2-heptadecanone. The data has been presented in Table 11. Similar protocol described earlier was followed during performing docking of these compounds with PLA2 (1KQU). From the table it was clear that generally compounds with higher binding affinities also possess higher inhibitory activities. The binding affinities and reported PLA2 inhibitory concentration of BA are − 41.00 kJ/mol and ~ 2.5 μM for 30% & ~ 5 μM for 40% [5] inhibition which is consistent in accordance to our findings of binding affinity and in vitro inhibitory activity.

Conclusions

The acid dissociation constant (pKa), distribution coefficient (logD), partition coefficient (logP), aqueous solubility (logS), solvation free energy, dipole moment, polarizability, hyperpolarizability and different reactivity descriptors such as the chemical potential, electrophilicity, chemical hardness and chemical softness of betulinic acid have been calculated using MarvinSketch 15.6.29 and Gaussian 09 software. The calculated properties showed that betulinic acid has three species (one unionized and two ionized) over the pH range of 0.0 to 14.0 suggesting the unionized form is likely to exist in the acidic pH of the stomach however the betulinate form (ionized form) would be the predominant form in the alkaline pH of the intestine.

The logP, logD and logS values suggest that betulinic acid is non-polar and hydrophobic. This property would enable betulinic acid to pass through the lipid bilayer membrane of the cells. This hypothesis was corroborated by the results of HIA and permeability of betulinic acid through Caco-2 cell. It was found that BA has low skin permeability hence topical application BA as an anti-inflammatory agent can be achieved. Further, being lipophilic in nature betulinic acid would also exhibit positive CNS activity due to high permeability through BBB as evident from our in silico data.

The computational investigation of solvation free energy in different solvents explains the relative stability or reactivity of betulinic acid. Our theoretical calculation

Table 10 Binding affinity (kJ/mol) and interactions of BR4 and BA with phospholipase A2 (1KQU)

Compound Name	Binding affinity (kJ/mol)	Amino acid and ligand (BR4/BA) interactions	Bond Distances (Å)	Category of interaction	Types of interaction
6-Phenyl-4(R)-(7-Phenyl-heptanoylamino)-hexanoic acid (BR4)	−33.89	LYS62[H…O]BR4	2.870	Hydrogen Bond;Electrostatic	Salt Bridge; Attractive Charge
		$[Ca^{+2}$…O]BR4	4.024	Electrostatic	Attractive Charge
		BR4[NH…N]HIS47	1.829	Hydrogen Bond	Conventional Hydrogen Bond
		GLY29[NH…O]BR4	1.796	Hydrogen Bond	Conventional Hydrogen Bond
		GLY31[NH…O]BR4	2.374	Hydrogen Bond	Conventional Hydrogen Bond
		CYS28[H…O]BR4	2.601	Hydrogen Bond	Carbon Hydrogen Bond
		VAL30[H…O]BR4	2.388	Hydrogen Bond	Carbon Hydrogen Bond
		LYS62[H…O]BR4	2.941	Hydrogen Bond	Carbon Hydrogen Bond
		$[Ca^{+2}$…O]BR4	2.767	Other	Metal-Acceptor
		$[Ca^{+2}$…O]BR4	2.489	Other	Metal-Acceptor
		BR4[Pi…Pi]BR4	4.726	Hydrophobic	Pi-Pi T-shaped
		GLY29-VAL30[CON…BR4]	4.326	Hydrophobic	Amide-Pi Stacked
		BR4[Pi…Alkyl]LEU2	4.891	Hydrophobic	Pi-Alkyl
		BR4[Pi…Alkyl]ALA17	4.480	Hydrophobic	Pi-Alkyl
		BR4[Pi…Alkyl]ALA18	5.058	Hydrophobic	Pi-Alkyl
		BR4[Pi…Alkyl]LEU2	4.483	Hydrophobic	Pi-Alkyl
Betulinic acid (BA)	−41.00	GLY22[H…O]BA	2.493	Hydrogen Bond	Carbon Hydrogen Bond
		GLY29[H…O]BA	2.714	Hydrogen Bond	Carbon Hydrogen Bond
		BA[Pi…Sigma]PHE5	3.783	Hydrophobic	Pi-Sigma
		BA[Alkyl…Alkyl]LEU2	5.406	Hydrophobic	Alkyl
		BA[Alkyl…Alkyl]LEU2	4.322	Hydrophobic	Alkyl
		BA[Alkyl…Alkyl]ALA18	3.715	Hydrophobic	Alkyl
		BA[Alkyl…Alkyl]LEU2	3.813	Hydrophobic	Alkyl
		BA[Alkyl…Alkyl]ALA18	3.870	Hydrophobic	Alkyl
		BA[Alkyl…Alkyl]ALA18	3.892	Hydrophobic	Alkyl
		BA[Alkyl…Alkyl]LEU2	4.924	Hydrophobic	Alkyl
		LEU2[Alkyl…Alkyl]BA	3.962	Hydrophobic	Alkyl
		ALA17[Alkyl…Alkyl]BA	5.402	Hydrophobic	Alkyl
		ALA17[Alkyl…Alkyl]BA	5.356	Hydrophobic	Alkyl
		ALA18[Alkyl…Alkyl]BA	3.737	Hydrophobic	Alkyl
		PHE5[Pi…Alkyl]BA	5.290	Hydrophobic	Pi-Alkyl
		PHE5[Pi…Alkyl]BA	4.239	Hydrophobic	Pi-Alkyl
		HIS6[Pi…Alkyl]BA	5.133	Hydrophobic	Pi-Alkyl
		HIS6[Pi…Alkyl]BA	4.162	Hydrophobic	Pi-Alkyl
		HIS47[Pi…Alkyl]BA	5.074	Hydrophobic	Pi-Alkyl
		HIS47[Pil…Alkyl]BA	5.073	Hydrophobic	Pi-Alkyl
		TYR51[Pi…Alkyl]BA	4.321	Hydrophobic	Pi-Alkyl

Table 11 Binding affinities (kJ/mol) and in vitro inhibitory activity (IC_{50}) of different PLA2 inhibitors

Compound name	IC_{50} (μM) [86–88]	Binding affinity (kJ/mol)
LY 311727	< 1	−39.75
Manoalide	16	−39.33
Indomethacin	35	−36.82
Manoalogue	26	−34.31
Aristolochic Acid	40	−33.89
1,1,1-Trifluoro-2-heptadecanone	45	−27.20

suggests that betulinic acid stabilized more in non-polar protic solvent due to hydrophobic interaction between the steroidal nucleus with the non-polar region of solvent and the electrostatic interaction between carboxyl group of betulinic acid with the polar portion of the solvent. Due to greater interaction with non-polar solvent the HOMO-LUMO gap becomes shorter as compared to the polar solvent (Table 5 and Fig. 11). It could also be inferred that it is this property which facilitates the hydrophobic interactions and formation of hydrogen bond of BA at the binding site cavity of PLA2.

BA was found to have 100% plasma protein binding and hence it could be deduced that it is unlikely to be eliminated promptly from the systemic circulation upon administration. Since BA acts as both inhibitor and substrate for P glycoprotein due to complex modulatory interactions with the Pgp [83], it is unlikely to be pumped out of the cells completely hence reducing the possibility of resistance mediated by efflux pump.

BA is likely to be metabolized by Cytochrome P450 3A4. However, it must be noted that it is an inhibitor for the same enzyme which could be overcome with the administration of Cytochrome P450 3A4 inducer. Since BA was also found to be an inhibitor of Cytochrome P450 2C9, it should not be used when a drug (which acts as a substrate for this enzyme) needs to be metabolized.

The toxicological study revealed that although betulinic acid is a mutagenic compound, it was noncarcinogenic in mice model. Moreover, molecular docking study revealed that betulinic acid interacts with GLY22 & GLY29 through hydrogen bond formation and LEU2, PHE5, HIS6, ALA17, ALA18, HIS47 and TYR51 through different types of hydrophobic interactions with a binding affinity of – 41.00 kJ/mol.

These computed molecular properties may assist to develop analytical method [46] to assay BA and the pharmacokinetic, toxicology and molecular docking study may provide a guide to synthesize betulinic acid derivatives with better pharmacokinetic & toxicological properties with potent phospholipase A2 inhibitory activity.

Abbreviations

BA: Betulinic acid; BR4: 6-Phenyl-4(R)-(7-Phenyl-heptanoylamino)-hexanoic acid; DMSO: Dimethyl sulfoxide; HOMO: Highest occupied molecular orbital; LUMO: Lowest unoccupied molecular orbital; PDB: Protein Data Bank; PLA2: phospholipase A2; RMSD: Root mean square deviation; SMD: Solvation Model on Density

Acknowledgements

We would like to thank Dr. Shahidul M. Islam, Department of Chemistry, College of Science, Sultan Qaboos University for his help to conduct the research.

Funding

One of us (MAR) is thankful to the Ministry of Education, Government of the People's Republic of Bangladesh for a research grant (No. 37.01.0000.078.02.018.13–125/10/2/2015) for the period 2014–15 to 2016–17 to carry out the work.

Availability of data and materials

Data and material are included in the article.

Authors' contributions

Conceived and designed the experiments: MFK. Performed theoretical investigations: MFK, RBR, and AC. Analyzed the data: MFK, NN. Wrote the manuscript: MFK, RBR and MAR. All authors read and approved the final manuscript for publication.

Ethics approval and consent to participate

Not applicable.

Consent for publication

Not applicable.

Competing interests

The authors declare that there is no competing interest.

Publisher's Note

Author details

[1]Department of Pharmacy, State University of Bangladesh, Dhaka 1205, Bangladesh. [2]Department of Chemistry, Rajshahi University of Engineering and Technology, Rajshahi, Bangladesh. [3]Department of Pharmaceutical Chemistry, University of Dhaka, Dhaka 1000, Bangladesh.

Received: 2 June 2017 Accepted: 26 January 2018
Published online: 02 February 2018

References

1. Carvalho BM, Santos JD, Xavier BM, Almeida JR, Resende LM, Martins W, Marcussi S, Marangoni S, Stábeli RG, Calderon LA, Soares AM. Snake venom PLA2s inhibitors isolated from Brazilian plants: synthetic and natural molecules. Biomed Res Int. 2013;2013:1–8.
2. Fujoka T, Kashiwada Y, Robert EK. Anti-AIDS agents. Betulinic acid and platanic acid as anti-HIV principles from Syzygium claviflorum and the anti-HIV activity of structurally related triterpenoids. J Nat Prod. 1994;57:243–7.
3. Kashiwada Y, Wang HK, Nagao T, Kitanaka S, Yasuda I, Fujioka T, Yamagishi T, Cosentino LM, Kozuka M, Okabe H, Ikeshiro Y. Anti-AIDS agents. 30. Anti-HIV activity of oleanolic acid, pomolic acid, and structurally related triterpenoids 1. J Nat Prod. 1998;61(9):1090–5.
4. Bringmann G, Saeb W, Assi LA, Francois G, Narayanan AS, Peters K, Peters EM. Betulinic acid: isolation from Triphyophyllum peltatum and Ancistrocladus heyneanus, antimalarial activity, and crystal structure of the benzyl ester. Planta Med. 1997;63(03):255–7.
5. Bernard P, Scior T, Didier B, Hibert M, Berthon JY. Ethnopharmacology and bioinformatic combination for leads discovery: application to phospholipase a 2 inhibitors. Phytochemistry. 2001;58(6):865–74.
6. Huguet AI, del Carmen RM, Máñez S, Giner RM. Ríos JL. Effect of triterpenoids on the inflammation induced by protein kinase C activators, neuronally acting irritants and other agents. Eur J Pharmacol. 2000;410(1):69–81.

7. Mukherjee PK, Saha K, Das J, Pal M, Saha BP. Studies on the anti-inflammatory activity of rhizomes of Nelumbo Nucifera. Planta Med. 1997; 63(04):367–9.
8. Enwerem NM, Okogun JI, Wambebe CO, Okorie DA, Akah PA. Anthelmintic activity of the stem bark extracts of Berlina grandiflora and one of its active principles, Betulinic acid. Phytomedicine. 2001;8(2):112–4.
9. Kinoshita K, Akiba M, Saitoh M, Ye Y, Koyama K, Takahashi K, Kondo N, Yuasa H. Antinociceptive effect of triterpenes from cacti. Pharm Biol. 1998;36(1):50–5.
10. Ryu SY, Lee CK, Lee CO, Kim HS, Zee OP. Antiviral triterpenes from Prunella vulgaris. Arch Pharm Res. 1992;15(3):242–5.
11. Ryu SY, Lee CK, Ahn JW, Lee SH, Zee OP. Antiviral activity of triterpenoid derivatives. Arch Pharm Res. 1993;16(4):339–42.
12. Fulda S, Jeremias I, Steiner HH, Pietsch T, Debatin KM. Betulinic acid: a new cytotoxic agent against malignant brain-tumor cells. Int J Cancer. 1999;82(3):435–41.
13. Fulda S, Debatin KM. Betulinic acid induces apoptosis through a direct effect on mitochondria in neuroectodermal tumors. Med Pediatr Oncol. 2000;35(6):616–8.
14. Zuco V, Supino R, Righetti SC, Cleris L, Marchesi E, Gambacorti-Passerini C, Formelli F. Selective cytotoxicity of betulinic acid on tumor cell lines, but not on normal cells. Cancer Lett. 2002;175(1):17–25.
15. Cichewicz RH, Kouzi SA. Chemistry, biological activity, and chemotherapeutic potential of betulinic acid for the prevention and treatment of cancer and HIV infection. Med Res Rev. 2004;24(1):90–114.
16. O'Connell MM, Bentley MD, Campbell CS, Cole BJ. Betulin and lupeol in bark from four white-barked birches. Phytochemistry. 1988;27(7):2175–6.
17. Cole BJ, Bentley MD, Hua Y. Triterpenoid extractives in the outer bark of *Betula lenta* (black birch). Holzforschung. 1991;45(4):265–8.
18. Chowdhury A, Alam MA, Rashid RB, Al-Mansur MA, Rahman MS, Rashid MA. Steroids and triterpenoids from *Corypha taliera* Roxb: a critically endangered palm species of Bangladesh. Res J Med Plant. 2013;7:125–9.
19. Jagadeesh SG, Krupadanam GD, Srimannarayana G, Murthy SS, Kaur A, Raja SS. Tobacco caterpillar antifeedent from the gotti stem wood triterpene betulinic acid. J Agric Food Chem. 1998;46(7):2797–9.
20. Schühly W, Heilmann J, Calis I, Sticher O. New triterpenoids with antibacterial activity from Zizyphus joazeiro. Planta Med. 1999;65(08):740–3.
21. Chang CW, Wu TS, Hsieh YS, Kuo SC, Chao PD. Terpenoids of Syzygium Formosanum. J Nat Prod. 1999;62(2):327–8.
22. del Carmen RM, Giner RM, Manez S, Gueho J, Julien HR, Hostettmann K, Rios JL. Investigations on the steroidal anti-inflammatory activity of triterpenoids from Diospyros Leucomelas. Planta Med. 1995;61(01):9–12.
23. Singh P, Sharma S. Triterpenoid constituents of the seeds of *Diospyros melanoxylon*, *Tecomella undulata* and *Terminalia bellirica*. J Indian Chem Soc. 1997;74(6):504–5.
24. Lin HC, Ding HY, Wu YC. Two novel compounds from Paeonia s uffruticosa. J Nat Prod. 1998;61(3):343–6.
25. Krasutsky PA. Birch bark research and development. Nat Prod Rep. 2006; 23(6):919–42.
26. Wada SI, Tanaka R. Betulinic acid and its derivatives, potent DNA topoisomerase II inhibitors, from the bark of Bischofia Javanica. Chem Biodivers. 2005;2(5):689–94.
27. Reutrakul V, Chanakul W, Pohmakotr M, Jaipetch T, Yoosook C, Kasisit J, Napaswat C, Santisuk T, Prabpai S, Kongsaeree P, Tuchinda P. Anti-HIV-1 constituents from leaves and twigs of Cratoxylum arborescens. Planta Med. 2006;72(15):1433–5.
28. Steele JP, Warhurst DC, Kirby GC, Simmonds MJ. In vitro and in vivo evaluation of betulinic acid as an antimalarial. Phytother Res. 1999; 13(2):115–9.
29. Zhang Z, ElSohly HN, Jacob MR, Pasco DS, Walker LA, Clark AM. Natural products inhibiting Candida Albicans secreted aspartic proteases from Tovomita krukovii. Planta Med. 2002;68(01):49–54.
30. Domínguez-Carmona DB, Escalante-Erosa F, García-Sosa K, Ruiz-Pinell G, Gutierrez-Yapu D, Chan-Bacab MJ, Giménez-Turba A, Peña-Rodríguez LM. Antiprotozoal activity of betulinic acid derivatives. Phytomedicine. 2010; 17(5):379–82.
31. Ma J, Starck SR, Hecht SM. DNA polymerase β inhibitors from Tetracera boiviniana. J Nat Prod. 1999;62(12):1660–3.
32. Choi JY, Na M, Hyun Hwang I, Ho Lee S, Young Bae E, Yeon Kim B, Seog AJ. Isolation of betulinic acid, its methyl ester and guaiane sesquiterpenoids with protein tyrosine phosphatase 1B inhibitory activity from the roots of Saussurea Lappa CB Clarke. Molecules. 2009;14(1):266–72.
33. Nyasse B, Nono JJ, Nganso Y, Ngantchou I, Schneider B. Uapaca genus (Euphorbiaceae), a good source of betulinic acid. Fitoterapia. 2009;80(1):32–4.
34. Wenzig EM, Widowitz U, Kunert O, Chrubasik S, Bucar F, Knauder E, Bauer R. Phytochemical composition and in vitro pharmacological activity of two rose hip (Rosa Canina L.) preparations. Phytomedicine. 2008;15(10):826–35.
35. Costa JF, Barbosa-Filho JM, de Azevedo Maia GL, Guimarães ET, Meira CS, Ribeiro-dos-Santos R, de Carvalho LC, Soares MB. Potent anti-inflammatory activity of betulinic acid treatment in a model of lethal endotoxemia. Int Immunopharmacol. 2014;23(2):469–74.
36. Kim KS, Lee DS, Kim DC, Yoon CS, Ko W, Oh H, Kim YC. Anti-inflammatory effects and mechanisms of action of coussaric and betulinic acids isolated from *Diospyros kaki* in lipopolysaccharide-stimulated RAW 264.7 macrophages, 2016. Molecules. 21(9):1206.
37. Blaževski J, Petković F, Momčilović M, Paschke R, Kaluđerović GN, Stojković MM, Miljković D. Betulinic acid regulates generation of neuroinflammatory mediators responsible for tissue destruction in multiple sclerosis in vitro. Acta Pharmacol Sin. 2013;34(3):424–31.
38. Ong WY, Farooqui T, Kokotos G, Farooqui AA. Synthetic and natural inhibitors of phospholipases A2: their importance for understanding and treatment of neurological disorders. ACS Chem Neurosci. 2015;6(6):814–31.
39. Irvine RF. How is the level of free arachidonic acid controlled in mammalian cells? Biochem J. 1982;204(1):3.
40. Mayer RJ, Marshall LA. New insights on mammalian phospholipase A2 (s); comparison of arachidonoyl-selective and-nonselective enzymes. FASEB J. 1993;7(2):339–48.
41. Posadas I, Terencio MC, De Rosa S, Payá M. Cavernolide: a new inhibitor of human sPLA2 sharing unusual chemical features. Life Sci. 2000;67(24):3007–14.
42. Friess H, Shrikhande S, Riesle E, Kashiwagi M, Baczako K, Zimmermann A, Uhl W, Büchler MW. Phospholipase A2 isoforms in acute pancreatitis. Ann Surg. 2001;233(2):204–12.
43. Dennis EA, Rhee SG, Billah MM, Hannun YA. Role of phospholipase in generating lipid second messengers in signal transduction. FASEB J. 1991; 5(7):2068–77.
44. Clark JD, Milona N, Knopf JL. Purification of a 110-kilodalton cytosolic phospholipase A2 from the human monocytic cell line U937. Proc Natl Acad Sci U S A. 1990;87(19):7708–12.
45. Malleda C, Ahalawat N, Gokara M, Subramanyam R. Molecular dynamics simulation studies of betulinic acid with human serum albumin. J Mol Model. 2012;18(6):2589–97.
46. Khan MF, Rita SA, Kayser MS, Islam MS, Asad S, Rashid RB, Bari MA, Rahman MM, Al Aman DA, Setu NI, Banoo R. Theoretically guided analytical method development and validation for the estimation of rifampicin in a mixture of isoniazid and pyrazinamide by UV spectrophotometer. Front Chem. 2017; 5(27):1–12.
47. Bach RD, Ayala PY, Schlegel HB. A reassessment of the bond dissociation energies of peroxides. An ab initio study. J Am Chem Soc. 1996;118(50):12758–65.
48. Glukhovtsev MN, Bach RD. Ab initio study on the thermochemistry of vinyl radical and cation. Chem Phys Lett. 1998;286(1):51–5.
49. Abboud JL, Castano O, Dávalos JZ, Gomperts R. The standard enthalpies of formation of 1-and 2-Adamantyl cations and radicals. An ab initio study. Chem Phys Lett. 2001;337(4):327–30.
50. Li ZH, Wong MW. Scaling of correlation basis set extension energies. Chem Phys Lett. 2001;337(1):209–16.
51. Espinosa-García J. Theoretical C–H bond dissociation enthalpies for CH 3 OCl and CH 3 OBr. Chem Phys Lett 2000;316(5):563-568.
52. BecNe AD. Densityüfunctional thermochemistry. Ill. The role of exact exchange. J Chem Phys. 1993;98:5648–52.
53. Frisch MJ, Trucks GW, Schlegel HB, Scuseria GE, Robb MA, Cheeseman JR, Scalmani G, Barone V, Mennucci B, Petersson GA, Nakatsuji H. Fox DJ Gaussian 09, revision a. 02. Wallingford, CT: Gaussian. Inc.; 2009.
54. Marenich AV, Cramer CJ, Truhlar DG. Universal solvation model based on solute electron density and on a continuum model of the solvent defined by the bulk dielectric constant and atomic surface tensions. J Phys Chem B. 2009;113(18):6378–96.
55. Hansford KA, Reid RC, Clark CI, Tyndall JD, Whitehouse MW, Guthrie T, McGeary RP, Schafer K, Martin JL, Fairlie DP. D-tyrosine as a Chiral Precusor to potent inhibitors of human nonpancreatic Secretory Phospholipase A2 (IIa) with Antiinflammatory activity. Chembiochem. 2003;4(2–3):181–5.

56. Sánchez-Linares I, Pérez-Sánchez H, Cecilia JM, García JM. High-throughput parallel blind virtual screening using BINDSURF. BMC Bioinf. 2012;13(14):S13.
57. Imbernón B, Cecilia JM, Pérez-Sánchez H, Giménez D. METADOCK: A parallel metaheuristic schema for virtual screening methods. Int J High Perform Comput Appl. 2017; p. 1–15.
58. Cerón-Carrasco JP, Cerezo J, Requena A, Zuñiga J, Contreras-García J, Chavan S, Manrubia-Cobo M, Pérez-Sánchez H. Labelling Herceptin with a novel oxaliplatin derivative: a computational approach towards the selective drug delivery. J Mol Model. 2014;20(9):2401.
59. Navarro-Fernández J, Pérez-Sánchez H, Martínez-Martínez I, Meliciani I, Guerrero JA, Vicente V, Corral J, Wenzel W. In silico discovery of a compound with nanomolar affinity to antithrombin causing partial activation and increased heparin affinity. J Med Chem. 2012;55(14):6403–12.
60. Trott O, Olson AJ. AutoDock Vina: improving the speed and accuracy of docking with a new scoring function, efficient optimization, and multithreading. J Comput Chem. 2010;31(2):455–61.
61. Elusiyan CA, Msagati TA, Shode FO, Mamba BB. Measurements of distribution coefficients and lipophilicity values for oleanolic acid and betulinic acid extracted from indigenous plants by hollow fibre supported liquid membrane. Bull Chem Soc Ethiop. 2011;25(3):321–32.
62. Claude B, Morin P, Lafosse M, Andre P. Evaluation of apparent formation constants of pentacyclic triterpene acids complexes with derivatized β-and γ-cyclodextrins by reversed phase liquid chromatography. J Chromatogr A. 2004;1049(1):37–42.
63. Suhasini M, Sailatha E, Gunasekaran S, Ramkumaar GR. Vibrational and electronic investigations, thermodynamic parameters, HOMO and LUMO analysis on Lornoxicam by density functional theory. J Mol Struct. 2015; 1100:116–28.
64. Chattaraj PK, Maiti B, Sarkar U. Philicity: a unified treatment of chemical reactivity and selectivity. J Phys Chem A. 2003;107(25):4973–5.
65. Parr RG, Donnelly RA, Levy M, Palke WE. Electronegativity: the density functional viewpoint. J Chem Phys. 1978;68(8):3801–7.
66. Parr RG, Pearson RG. Absolute hardness: companion parameter to absolute electronegativity. J Am Chem Soc. 1983;105(26):7512–6.
67. Parr RG, Chattaraj PK. Principle of maximum hardness. J Am Chem Soc. 1991;113(5):1854–5.
68. Parr RG, Szentpaly LV, Liu S. Electrophilicity index. J Am Chem Soc. 1999; 121(9):1922–4.
69. Yee S. In vitro permeability across Caco-2 cells (colonic) can predict in vivo (small intestinal) absorption in man—fact or myth. Pharm Res. 1997;14(6):763–6.
70. Yazdanian M, Glynn SL, Wright JL, Hawi A. Correlating partitioning and Caco-2 cell permeability of structurally diverse small molecular weight compounds. Pharm Res. 1998;15(9):1490–4.
71. Singh S, Singh J. Transdermal drug delivery by passive diffusion and iontophoresis: a review. Med Res Rev. 1993;13(5):569–621.
72. Chen C, Yang J. Predictive model of blood-brain barrier penetration of organic compounds. Acta Pharmacol Sin. 2005;26(4):500–12.
73. Tanaka H, Mizojiri K. Drug-protein binding and blood-brain barrier permeability. J Pharmacol Exp Ther. 1999;288(3):912–8.
74. Cornford EM, Pardridge WM, Braun LD, Oldendorf WH. Increased blood-brain barrier transport of protein-bound anticonvulsant drugs in the newborn. J Cereb Blood Flow Metab. 1983;3(3):280–6.
75. Pardridge WM, Sakiyama R, Fierer G. Transport of propranolol and lidocaine through the rat blood-brain barrier. Primary role of globulin-bound drug. J Clin Invest. 1983;71(4):900.
76. Terasaki TE, Pardridge WM, Denson DD. Differential effect of plasma protein binding of bupivacaine on its in vivo transfer into the brain and salivary gland of rats. J Pharmacol Exp Ther. 1986;239(3):724–9.
77. Schinkel AH. P-glycoprotein, a gatekeeper in the blood–brain barrier. Adv Drug Deliv Rev. 1999;36(2):179–94.
78. Cabrera MA, González I, Fernández C, Navarro C, Bermejo M. A topological substructural approach for the prediction of P-glycoprotein substrates. J Pharm Sci. 2006;95(3):589–606.
79. Kim RB, Fromm MF, Wandel C, Leake B, Wood AJ, Roden DM, Wilkinson GR. The drug transporter P-glycoprotein limits oral absorption and brain entry of HIV-1 protease inhibitors. J Clin Invest. 1998;101(2):289.
80. de Cerqueira LP, Golbraikh A, Oloff S, Xiao Y, Tropsha A. Combinatorial QSAR modeling of P-glycoprotein substrates. J Chem Inf Model. 2006;46(3):1245–54.
81. Wang YH, Li Y, Yang SL, Yang L. Classification of substrates and inhibitors of P-glycoprotein using unsupervised machine learning approach. J Chem Inf Model. 2005;45(3):750–7.
82. Joung JY, Kim HJ, Kim HM, Ahn SK, Nam KY, No KT. Prediction models of p-glycoprotein substrates using simple 2d and 3d descriptors by a recursive partitioning approach. Bull Kor Chem Soc. 2012;33(4):1123–7.
83. Zhou SF. Drugs behave as substrates, inhibitors and inducers of human cytochrome P450 3A4. Curr Drug Metab. 2008;9(4):310–22.
84. Sanguinetti MC, Tristani-Firouzi M. hERG potassium channels and cardiac arrhythmia. Nature. 2006;440(7083):463–9.
85. Krieger E, Joo K, Lee J, Lee J, Raman S, Thompson J, Tyka M, Baker D, Karplus K. Improving physical realism, stereochemistry, and side-chain accuracy in homology modeling: four approaches that performed well in CASP8. Proteins. 2009;77(S9):114–22.
86. Lister MD, Glaser KB, Ulevitch RJ, Dennis EA. Inhibition studies on the membrane-associated phospholipase A2 in vitro and prostaglandin E2 production in vivo of the macrophage-like P388D1 cell. Effects of manoalide, 7, 7-dimethyl-5, 8-eicosadienoic acid, and p-bromophenacyl bromide. J Biol Chem. 1989;264(15):8520–8.
87. Lobo IB, Hoult JR. Groups I, II and III extracellular phospholipases A2: selective inhibition of group II enzymes by indomethacin but not other NSAIDs. Agents Actions. 1994;41(1–2):111–3.
88. Santa Cruz Biotechnology. https://www.scbt.com/scbt/browse/chemicals-Protein-Interacting-Inhibitors-Activators-Substrates-protein-inhibitors-pla2-inhibitors/_/N-16mpppv. Access Date: 13 May 2017.